Layer undulations induced by a magnetic or electric field in concentric cylindrical layers of smectic-*A* liquid crystals

I. W. Stewart*
Department of Mathematics, University of Strathclyde, Livingstone Tower, 26 Richmond Street, Glasgow G1 1XH, United Kingdom
(Received 25 January 1999)

This paper derives theoretical results for the onset of Helfrich-Hurault-type transitions in samples of smectic-*A* liquid crystals arranged in concentric cylindrical layers [J. Chem. Phys. **55**, 839 (1971); **59**, 2068 (1973)]. A magnetic field is applied in the azimuthal direction, parallel to the layers. The governing equilibrium equation is solved in order to derive the critical magnitude H_c of the magnetic field above which the onset of periodic smectic layer distortions is expected. The distortion solution is shown to be energetically favorable for $H>H_c$. Some examples of critical thresholds are given, by means of figures, for relevant physical parameters. The qualitative features of the solution at H_c are displayed via the plot of a typical variable solution to the equilibrium equation in a particular case. The consequences of the results, especially the relationship between H_c and the radial depth, are explored, and comparisons are drawn with known results for infinite planar aligned smectic-*A* samples. The results are also interpreted for the case of an electric field which follows the plane of the layers in the usual wedge geometry. Critical applied voltage magnitudes U_c are derived for various radial sample depths and wedge angles. [S1063-651X(99)13708-5]

PACS number(s): 61.30.Cz, 87.22.−q

I. INTRODUCTION

This paper extends the work of Helfrich [1] and Hurault [2] for infinite samples of cholesteric liquid crystals under the influence of a magnetic field to samples of concentric cylindrical layers of smectic-*A* liquid crystals. Theoretical results for the Helfrich-Hurault transition are well known for infinite samples of planar aligned smectic-*A* liquid crystals under the application of a magnetic field: at a critical magnitude of the field strength the smectic layers begin to distort or undulate, resulting in one- or two-dimensional patterns. Details of this effect, and on the general properties of smectic liquid crystals, can be found in de Gennes and Prost [3] or Chandrasekhar [4]. The present aim is to examine theoretically the possibility for the onset of a Helfrich-Hurault-type transition for concentric cylindrical smectic-*A* layers, where the magnetic field is locally parallel to the cylindrical layers but perpendicular to their common axis; the details of this geometry are discussed below.

Smectic-*A* liquid crystals are layered anisotropic fluids. Each layer consists of long molecules whose average molecular alignment is locally perpendicular to the layers. This average alignment is denoted by the unit vector **n**, called the director, and it is well known that there are six types of well behaved surfaces, corresponding to the layers, which provide static equilibrium configurations. These are the Dupin cyclides [5–7], parabolic cyclides [8–11], circular tori of revolution [7], spheres [12], infinite cylinders [13,14], and planes. Our attention is restricted to infinite cylinders and, for the problem considered here, the sample alignment is shown in Fig. 1. The smectic layers are arranged in concentric equidistant cylinders whose common axis coincides with the z axis of the usual cylindrical polar coordinate system (r,α,z), with $\hat{\mathbf{r}}$, $\hat{\boldsymbol{\alpha}}$, and $\hat{\mathbf{z}}$ denoting the basis vectors in the r, α, and z directions, respectively. The initial average molecular alignment, denoted by $\mathbf{n}_0=\hat{\mathbf{r}}$ in Fig. 1, is perpendicular to the layers and coincident with the layer normal as indicated. This geometry has also been discussed in the context of cell membranes by Das and Schwarz [15]. It is assumed that the sample is infinite in the z direction, and that the smectic-*A* liquid crystal is in a homeotropic alignment contained between two cylindrical boundaries at the radial distances $r=a$ and $r=b$ as shown. A magnetic field is applied of the form

$$\mathbf{H}=\frac{Ha}{r}\hat{\boldsymbol{\alpha}}, \tag{1.1}$$

where H is the magnetic field strength at $r=a$. Such a field may be achieved by passing an electric current along a wire situated along the z axis. To derive the governing equilibrium equation for the director **n** when $H\neq 0$, we construct the

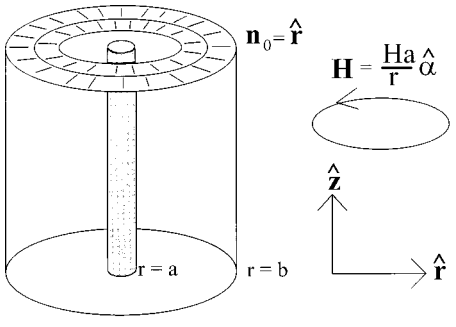

FIG. 1. The arrangement of concentric cylindrical smectic-*A* layers with inner radius a and outer radius b. The initial alignment of the director is $\mathbf{n}_0$, coincident with the unit radial vector $\hat{\mathbf{r}}$. The magnetic field **H** is in the azimuthal direction $\hat{\alpha}$, and is locally parallel to the layers.

*Electronic address; i.w.stewart@strath.ac.uk

bulk elastic and magnetic energies following the work by Kleman and Parodi [16], and then minimize the total energy via the appropriate Euler-Lagrange equation. The total energy, equilibrium equation, and boundary conditions are discussed in Sec. II. The equilibrium equation is solved in Sec. III, and a critical field strength H_c is derived for the onset of layer displacements. An energy comparison in Sec. IV further reveals that the solution for layer displacements is energetically favourable to the zero displacement solution when $H>H_c$. Some examples of solutions and critical field strengths for physically relevant parameters are examined in Sec. V. Section VI interprets the results in the previous sections in relation to an electric field applied across a wedge of cylindrical smectic-*A* layers, the field term in Eq. (1.1) being suitably modified. The results are particularly relevant for layer undulations near the critical field magnitudes. Section VII concludes the article with a discussion of the results.

II. ENERGIES AND EQUILIBRIUM EQUATION

The magnetic field is assumed to be unaffected by the fluid so that **H** given by Eq. (1.1) satisfies

$$\nabla\wedge\mathbf{H}=0, \quad \nabla\cdot\mathbf{H}=0. \tag{2.1}$$

It is well known that the magnetic energy can then be written as (ignoring a constant contribution to the energy which does not affect the alignment of **n**) (Ref. [3], p. 119),

$$w_m=-\tfrac{1}{2}\chi_a(\mathbf{n}\cdot\mathbf{H})^2, \tag{2.2}$$

where χ_a is the anisotropy of diamagnetic susceptibility of the liquid crystal. In this case χ_a is supposed positive, which indicates that the director **n** ''prefers'' to align parallel to the magnetic field. Given that the direction of the field is initially perpendicular to **n**, the director can only align more with the field if it tilts with respect to the layer normal, inducing layer compression. Given the results for planar samples [3,17], we expect to find analogous solutions which model undulations of the layers at a critical field strength $H_c>0$.

Small deviations in **n** from $\mathbf{n}_0$ will induce a displacement of the layers. This displacement is represented in the usual notation by $u(r,\alpha,z)$, with $|u|\ll 1$. For notational convenience we follow [16] and define

$$(\nabla_\perp u)^2=u_z^2+\frac{1}{r^2}u_\alpha^2, \tag{2.3}$$

$$\nabla_\perp^2 u=u_{zz}+\frac{1}{r^2}u_{\alpha\alpha}, \tag{2.4}$$

where subscripts denote partial derivatives with respect to the relevant variables. From Ref. [16] it is known that to second order in u we may write

$$\mathbf{n}=\left[1-\frac{1}{2}(\nabla_\perp u)^2\right]\hat{\mathbf{r}}-\frac{1}{r}u_\alpha(1+u_r)\hat{\boldsymbol{\alpha}}-u_z(1+u_r)\hat{\mathbf{z}}. \tag{2.5}$$

The usual smectic-*A* bulk elastic energy is (Ref. [4], pp. 98 and 310)

$$w_A=\frac{K_1}{2}(\nabla\cdot\mathbf{n})^2, \tag{2.6}$$

where $K_1>0$ is the splay elastic constant. The elastic energy corresponding to compression of the layers is (Ref. [16], p. 680)

$$w_L=\frac{\overline{B}}{2}u_r^2, \tag{2.7}$$

where $\overline{B}$ is the smectic layer compression constant. Substituting Eq. (2.5) into Eq. (2.6) yields the total elastic energy $w_{\rm el}$ in terms of u as (linear combinations in u are discounted due to symmetry considerations)

$$w_{\rm el}=w_L+w_A=\frac{\overline{B}}{2}u_r^2+\frac{K_1}{2}\left(\frac{1}{r^2}+(\nabla_\perp^2 u)^2-\frac{1}{r^2}(\nabla_\perp u)^2\right)+S, \tag{2.8}$$

where S is the surface term

$$S=-\frac{K_1}{r}\left(\frac{1}{2}\frac{\partial}{\partial r}(\nabla_\perp u)^2+\frac{1}{r^2}\frac{\partial}{\partial\alpha}(u_\alpha u_r)+\frac{\partial}{\partial z}(u_z u_r)\right). \tag{2.9}$$

A further substitution of Eq. (2.5) into Eq. (2.2) gives the magnetic energy (to second order in u)

$$w_m=-\frac{H^2a^2}{2r^4}\chi_a u_\alpha^2. \tag{2.10}$$

Ignoring surface contributions we finally arrive at the total energy of the system given by the sum $w=w_{\rm el}+w_m-S$ of the elastic and magnetic energies. Hence we take

$$w=\frac{\overline{B}}{2}u_r^2+\frac{K_1}{2}\left(\frac{1}{r^2}+(\nabla_\perp^2 u)^2-\frac{1}{r^2}(\nabla_\perp u)^2\right)-\frac{H^2a^2}{2r^4}\chi_a u_\alpha^2. \tag{2.11}$$

The total energy integral, in polar coordinates, over a unit depth in z, is

$$W=\int_\Omega w r\,dr\,d\alpha\,dz, \tag{2.12}$$

where Ω is the volume $a\leqslant r\leqslant b$, $0\leqslant\alpha\leqslant 2\pi$, $0\leqslant z\leqslant 1$. The Euler-Lagrange equation for extrema u of an integral whose integrand $\overline{w}$ depends on the function $u(x_1,x_2,x_3)$ and its derivatives up to second order (with no mixed derivatives) in the variables x_i, $i=1$, 2, and 3, is (Ref. [18], p. 202)

$$\frac{\partial\overline{w}}{\partial u}+\sum_{i=1}^{3}\left[\frac{\partial^2}{\partial x_i^2}\left(\frac{\partial\overline{w}}{\partial(u_{ii})}\right)-\frac{\partial}{\partial x_i}\left(\frac{\partial\overline{w}}{\partial u_i}\right)\right]=0, \tag{2.13}$$

where, for example, u_i denotes partial differentiation of u with respect to the ith variable. Setting $\overline{w}=wr$ in Eq. (2.13) gives the following governing static equilibrium equation for the energy W in Eq. (2.12)

$$K_1\nabla_\perp^2\left(\nabla_\perp^2+\frac{1}{r^2}\right)u+\frac{H^2a^2}{r^4}\chi_a u_{\alpha\alpha}=\bar{B}\frac{1}{r}\frac{\partial}{\partial r}(ru_r). \tag{2.14}$$

This is an extension of the equation discussed in Ref. [16]. The energy for each solution of Eq. (2.14) can be calculated via Eq. (2.12) and a comparison of energies is then possible. This comparison determines which solution is energetically favorable, the solution with the least energy being preferred.

III. SOLUTIONS FOR $u=u(r,\alpha)$

The simplest solutions can be found when z dependence is neglected. We shall assume the surface anchoring in the sample is such that $\mathbf{n}$ is equal to $\mathbf{n}_0=\hat{\mathbf{r}}$ on the boundaries at $r=a,b$. Solutions of the form

$$u(r,\alpha)=v(r)\sin(m\alpha), \tag{3.1}$$

with m an integer are sought, with the expectation that each cylindrical layer will undergo a periodic distortion in the $\hat{\boldsymbol{\alpha}}$ direction. The number m plays a similar rôle to that of the wave number considered in Ref. [3]. This is analogous to the periodic distortions reviewed in Refs. [3,4] for planar aligned smectic-*A* samples. The variable separable form for the solution in Eq. (3.1) is a standard ansatz for cylinder problems in liquid crystals [16]. The corresponding boundary conditions are

$$v(a)=v(b)=0. \tag{3.2}$$

The equilibrium equation (2.14) in this case becomes

$$\frac{K_1}{r^4}(u_{\alpha\alpha\alpha\alpha}+u_{\alpha\alpha})+\frac{H^2a^2}{r^4}\chi_a u_{\alpha\alpha}=\bar{B}\frac{1}{r}\frac{\partial}{\partial r}(ru_r). \tag{3.3}$$

Inserting the ansatz (3.1) into Eq. (3.3) and simplifying shows that the ordinary differential equation

$$r^2\frac{d^2v}{dr^2}+r\frac{dv}{dr}-\frac{\sigma^2(m,H)}{r^2}v=0 \tag{3.4}$$

must be satisfied with

$$\sigma^2(m,H)=\frac{m^2}{\bar{B}}(K_1(m^2-1)-\chi_a H^2a^2). \tag{3.5}$$

The quantity $\sigma^2(m,H)$ depends on the magnetic field strength H and may be positive, zero, or negative. We consider each case separately.

Case (i) $\sigma^2(m,H)\geqslant 0$. Making the change of variable

$$s=i\frac{|\sigma(m,H)|}{r},\quad i^2=-1, \tag{3.6}$$

in Eq. (3.4), noting that $s^2=-\sigma^2(m,H)/r^2$, gives Bessel's equation in the form

$$s^2\frac{d^2v}{ds^2}+s\frac{dv}{ds}+s^2v=0. \tag{3.7}$$

Hence the general solution to Eq. (3.7) is

$$v(s)=C_1J_0(s)+C_2Y_0(s), \tag{3.8}$$

where C_1 and C_2 are arbitrary constants and J_0 and Y_0 are Bessel functions of the first and second kinds, respectively, of order zero. For real η, the functions J_0 and Y_0 satisfy (Ref. [19], p. 375)

$$J_0(i\eta)=I_0(\eta), \tag{3.9}$$

$$Y_0(i\eta)=iI_0(\eta)-\frac{2}{\pi}K_0(\eta), \tag{3.10}$$

where I_0 and K_0 are the modified Bessel functions of the first and second kinds of order zero. The solution in terms of $v(r)$ can now be written as (with different constants C_1 and C_2)

$$v(r)=C_1I_0\left(\frac{|\sigma(m,H)|}{r}\right)+C_2K_0\left(\frac{|\sigma(m,H)|}{r}\right). \tag{3.11}$$

Applying the boundary conditions (3.2) shows that we require

$$\begin{bmatrix} I_0\left(\frac{|\sigma(m,H)|}{a}\right) & K_0\left(\frac{|\sigma(m,H)|}{a}\right) \\ I_0\left(\frac{|\sigma(m,H)|}{b}\right) & K_0\left(\frac{|\sigma(m,H)|}{b}\right)\end{bmatrix}\begin{bmatrix}C_1\\C_2\end{bmatrix}=\begin{bmatrix}0\\0\end{bmatrix}. \tag{3.12}$$

It is known (Ref. [19], pp. 374–376) that I_0 and K_0 have no real zeros and that $I_0'(\eta)=I_1(\eta)>0$ and $K_0'(\eta)=-K_1(\eta)<0$ for $\eta>0$. Hence

$$I_0\left(\frac{|\sigma(m,H)|}{a}\right)>I_0\left(\frac{|\sigma(m,H)|}{b}\right)>0,$$

$$K_0\left(\frac{|\sigma(m,H)|}{b}\right)>K_0\left(\frac{|\sigma(m,H)|}{a}\right)>0. \tag{3.13}$$

It follows that

$$I_0\left(\frac{|\sigma(m,H)|}{a}\right)K_0\left(\frac{|\sigma(m,H)|}{b}\right)-I_0\left(\frac{|\sigma(m,H)|}{b}\right)K_0\left(\frac{|\sigma(m,H)|}{a}\right)>0, \tag{3.14}$$

and therefore the determinant of the coefficients on the left-hand side of Eq. (3.12) is always nonzero. Thus $C_1=C_2=0$ is the only solution of Eq. (3.12), leading to $v(r)\equiv 0$ as the only solution to Eq. (3.4) with Eq. (3.2). This means that for $\sigma^2(m,H)>0$ there are no real nonzero solutions to the given boundary value problem.

When $\sigma^2(m,H)=0$, Eq. (3.4) is easily integrated to find $v(r)=C_1\ln r+C_2$, and a simple application of the boundary conditions again shows $v(r)\equiv 0$ to be the only real solution available. It is easily observed from Eq. (3.5) that when no field is present then $\sigma^2(m,0)\geqslant 0$ for all integers m and hence, from the above results only the zero solution is available. Thus the cylindrical layers, when constructed, are anticipated to prefer remaining cylindrical when no field is present.

Case (ii) $\sigma^2(m,H)<0$. It is first observed that $\sigma^2(m,H)<0$ for all $H>0$ when $m=\pm 1$. When $\sigma^2(m,H)<0$ we can make a similar change of variable to Eq. (3.6) by setting

$$s=\frac{|\sigma(m,H)|}{r}, \tag{3.15}$$

leading to Eq. (3.7) from Eq. (3.4) again, noting that $-\sigma^2(m,H)=|\sigma(m,H)|^2$. The solution corresponding to the analog of Eq. (3.8) is then, in the variable r,

$$v(r)=C_1 J_0\left(\frac{|\sigma(m,H)|}{r}\right)+C_2 Y_0\left(\frac{|\sigma(m,H)|}{r}\right). \tag{3.16}$$

As in Eq. (3.12), the boundary conditions (3.2) force the following to be satisfied for the constants C_1 and C_2:

$$\begin{bmatrix} J_0\left(\frac{|\sigma(m,H)|}{a}\right) & Y_0\left(\frac{|\sigma(m,H)|}{a}\right) \\ J_0\left(\frac{|\sigma(m,H)|}{b}\right) & Y_0\left(\frac{|\sigma(m,H)|}{b}\right) \end{bmatrix}\begin{bmatrix} C_1 \\ C_2 \end{bmatrix}=\begin{bmatrix} 0 \\ 0 \end{bmatrix}. \tag{3.17}$$

To simplify the discussion we introduce the parameters

$$\lambda=\frac{b}{a}>1, \quad q(m,H)=\frac{|\sigma(m,H)|}{b}. \tag{3.18}$$

The determinant $\det(\lambda,q(m,H))$ of the coefficient matrix in Eq. (3.17) is then

$$\det(\lambda,q(m,H))=J_0(\lambda q(m,H))Y_0(q(m,H)) - Y_0(\lambda q(m,H))J_0(q(m,H)). \tag{3.19}$$

For nonzero solutions C_1 and C_2 to Eq. (3.17) it is necessary to find the first zero of $\det(\lambda,q(m,H))$ for fixed $\lambda>1$, with $q(m,H)$ treated as a variable essentially dependent upon the magnetic field strength H (from the definition of q and σ). [It is worth remarking here that $v(r)$ can be zero inside the sample as well as on the boundaries: in such cases we can look for the second, third, or higher zeros of $\det(\lambda,q(m,H))$. As a first approximation, however, it is expected that a first zero will provide an adequate indication of the behavior near the critical threshold.] Let q_λ be the first zero of $\det(\lambda,q(m,H))$ for some fixed $\lambda>1$. Such a first zero exists and is positive by the results contained in Ref. [19], p. 415: such zeros have to be found numerically, although asymptotic formulas are available. It follows that H must satisfy $q_\lambda=|\sigma(m,H)|/b$, and hence

$$b^2 q_\lambda^2=-\sigma^2(m,H)=\frac{m^2}{\overline{B}}(\chi_a H^2 a^2-K_1(m^2-1)). \tag{3.20}$$

Since $b=\lambda a$, Eq. (3.20) can be rearranged to find that H satisfies

$$H=f(m)\equiv\frac{1}{a}\left(\frac{K_1}{\chi_a}\right)^{1/2}(m^2+Q_\lambda m^{-2}-1)^{1/2}, \tag{3.21}$$

where

$$Q_\lambda=\frac{\overline{B}}{K_1}a^2\lambda^2 q_\lambda^2. \tag{3.22}$$

The least value of H is then given via the function $f(m)$, which is at its minimum when $m=Q_\lambda^{1/4}$. However, m must be an integer and therefore H is minimized at either $m=[Q_\lambda^{1/4}]$ or $m=[Q_\lambda^{1/4}]+1$ where $[X]$ denotes the greatest integer less than or equal to X. If $0<Q_\lambda\leq 1$, then it is clear that $m=1$ gives the minimum value H_c found from Eq. (3.21) [$m=0$ is discounted because q_λ in Eq. (3.20) cannot be zero]. To ease notation, define

$$m_c=[Q_\lambda^{1/4}] \quad \text{for } Q_\lambda>1. \tag{3.23}$$

For $Q_\lambda>1$ the difference $f^2(m_c+1)-f^2(m_c)$ can be calculated to determine whether m_c or m_c+1 gives the minimum value of m to provide the minimum value H_c of $H=f(m)$. We have that

$$f^2(m_c+1)-f^2(m_c)=\frac{1}{a^2}\frac{K_1}{\chi_a}\frac{(2m_c+1)}{m_c^2(m_c+1)^2} \times(m_c^2(m_c+1)^2-Q_\lambda), \tag{3.24}$$

from which it easily follows that

$$H_c=\begin{cases} f(1)=\frac{1}{a}\left(\frac{K_1}{\chi_a}\right)^{1/2}Q_\lambda^{1/2} & \text{if } 0<Q_\lambda\leq 1, \\ f(m_c) & \text{if } Q_\lambda<m_c^2(m_c+1)^2, \\ f(m_c+1) & \text{if } Q_\lambda>m_c^2(m_c+1)^2. \end{cases} \tag{3.25}$$

The quantity Q_λ therefore characterizes the behavior of H_c. Further, from the property that $q_\lambda\to\infty$ as $\lambda\to 1^+$ (Ref. [19], p. 374), it is clear that $H_c\to\infty$ as $\lambda\to 1^+$, that is, as the radius ratio tends to unity. The quantity H_c therefore corresponds to the usual interpretation of a critical threshold for the onset of a Helfrich-Hurault-type transition.

The solution $u(r,\alpha)$ at $H=H_c$ is found from Eqs. (3.1) and (3.16), and the solution of Eq. (3.17) with $\det(\lambda,q(m,H))=0$. In this case, with $C_1=u_0$, $C_2=-u_0 J_0(|\sigma_c|/a)J_0/Y_0(|\sigma_c|/a)$, u_0 an arbitrary constant, the solutions are

$$u(r,\alpha)=u_0\frac{\sin(m\alpha)}{Y_0(|\sigma_c|/a)}V(r), \qquad V(r)=J_0\left(\frac{|\sigma_c|}{r}\right)Y_0\left(\frac{|\sigma_c|}{a}\right)-Y_0\left(\frac{|\sigma_c|}{r}\right)J_0\left(\frac{|\sigma_c|}{a}\right), \tag{3.26}$$

with

$$|\sigma_c|=|\sigma(m,H_c)|=bq_\lambda=a\lambda q_\lambda, \tag{3.27}$$

$$m=\begin{cases} 1 & \text{if } 0<Q_\lambda\leq 1, \\ m_c & \text{if } Q_\lambda\leq m_c^2(m_c+1)^2, \\ m_c+1 & \text{if } Q_\lambda>m_c^2(m_c+1)^2. \end{cases} \tag{3.28}$$

The nature of the solution then depends upon the quantity Q_λ in Eq. (3.22). It is worth noting that the zeros of J_0 and Y_0 do not generally coincide with the zeros of $\det(\lambda, q(m,H))$ so that the solution in Eq. (3.26) generally exists (this follows from the fact that J_0 and Y_0 have no common zeros). The energy associated with this solution is examined in Sec. IV, before some examples are given for physical parameters in Sec. V.

IV. ENERGY CONSIDERATIONS

The equilibrium equation (2.14) has both the solutions $u \equiv 0$ and $u(r,\alpha)$ in Eq. (3.26) satisfying the boundary conditions (3.2). As is common in liquid crystal theory, a comparison of the energies for such solutions determines which one is energetically favorable: the solution with the least energy is interpreted as the preferred physical solution. We set

$$\Delta W = W(u(r,\alpha)) - W(u \equiv 0), \tag{4.1}$$

with W being the total energy integral in Eq. (2.12), and consider the region $a \leqslant r \leqslant b$, $0 \leqslant \alpha \leqslant 2\pi$, $0 \leqslant z \leqslant 1$. For the solution $u(r,\alpha)$ in Eq. (3.26) it is found that

$$\left(\frac{dV}{dr}\right)^2 = \frac{|\sigma_c|^2}{r^4}\left(Y_1\left(\frac{|\sigma_c|}{r}\right)J_0\left(\frac{|\sigma_c|}{a}\right) - J_1\left(\frac{|\sigma_c|}{r}\right)Y_0\left(\frac{|\sigma_c|}{a}\right)\right)^2, \tag{4.2}$$

$$u_r^2 = u_0^2 \frac{\sin^2(m\alpha)}{Y_0^2(|\sigma_c|/a)}\left(\frac{dV}{dr}\right)^2, \tag{4.3}$$

$$(\nabla_\perp u)^2 = u_0^2 \frac{m^2}{r^2}\frac{\cos^2(m\alpha)}{Y_0^2(|\sigma_c|/a)}V^2(r), \tag{4.4}$$

$$(\nabla_\perp^2 u)^2 = u_0^2 \frac{m^4}{r^4}\frac{\sin^2(m\alpha)}{Y_0^2(|\sigma_c|/a)}V^2(r), \tag{4.5}$$

and hence

$$\begin{aligned}\Delta W &= \frac{1}{2}\int_a^b \int_0^{2\pi}\left[r\overline{B}u_r^2 + K_1 r\left((\nabla_\perp^2 u)^2 - \frac{1}{r^2}(\nabla_\perp u)^2\right) - \frac{H^2a^2}{r^3}\chi_a u_\alpha^2\right]dr\,d\alpha \\ &= \frac{\pi}{2}\frac{u_0^2}{Y_0^2(|\sigma_c|/a)}\int_a^b\left[r\overline{B}\left(\frac{dV}{dr}\right)^2 + \frac{1}{r^3}(K_1 m^2(m^2-1) - m^2H^2a^2\chi_a)V^2(r)\right]dr \\ &= \frac{\pi}{2}\frac{u_0^2\overline{B}}{Y_0^2(|\sigma_c|/a)}\int_a^b\left[r\left(\frac{dV}{dr}\right)^2 + \frac{\sigma^2}{r^3}V^2(r)\right]dr,\end{aligned} \tag{4.6}$$

where $\sigma = \sigma(m,H)$ is given by Eq. (3.5) above (the value of m appearing in σ_c, and σ is the same). To evaluate the integrals in Eq. (4.6) we begin by noting from Eq. (3.27) that $|\sigma_c|/b = q_\lambda$ and $|\sigma_c|/a = \lambda q_\lambda$. The substitution $x = |\sigma_c|/r$ then shows

$$\begin{aligned}&\int_a^b\left[r\left(\frac{dV}{dr}\right)^2 + \frac{\sigma^2}{r^3}V^2(r)\right]dr \\ &\quad = \int_{q_\lambda}^{\lambda q_\lambda} x\left[\left(\frac{dV}{dx}\right)^2 + \frac{\sigma^2}{|\sigma_c|^2}V^2(x)\right]dx,\end{aligned} \tag{4.7}$$

with

$$\frac{dV}{dx} = -J_1(x)Y_0(\lambda q_\lambda) + Y_1(x)J_0(\lambda q_\lambda). \tag{4.8}$$

Since V and dV/dx are cylinder functions (linear combinations of Bessel functions) of orders zero and 1, respectively, we employ the result from Watson (Ref. [20], p. 135) that for any cylinder function C_μ of order μ

$$\int x C_\mu^2(x)dx = \tfrac{1}{2}x^2(C_\mu^2(x) - C_{\mu-1}(x)C_{\mu+1}(x)), \tag{4.9}$$

ignoring constants of integration. Application of this result gives, noting that $J_{-1}(x) = -J_1(x)$, $J_0'(x) = -J_1(x)$, and similar results hold for Y_0 and Y_1,

$$\int x\left(\frac{dV}{dx}\right)^2 dx = \frac{1}{2}x^2\left(\frac{dV}{dx}\right)^2 - \frac{1}{2}x^2V(x)[Y_0(\lambda q_\lambda)J_2(x) - J_0(\lambda q_\lambda)Y_2(x)] \tag{4.10}$$

$$\begin{aligned}\int x V^2(x)dx &= \frac{1}{2}x^2V^2(x) - \frac{1}{2}x^2[Y_0(\lambda q_\lambda)J_{-1}(x) - J_0(\lambda q_\lambda)Y_{-1}(x)][Y_0(\lambda q_\lambda)J_1(x) - J_0(\lambda q_\lambda)Y_1(x)] \\ &= \frac{1}{2}x^2V^2(x) + \frac{1}{2}x^2\left(\frac{dV}{dx}\right)^2.\end{aligned} \tag{4.11}$$

From the boundary conditions, $V(\lambda q_\lambda) = V(q_\lambda) = 0$, and hence from Eqs. (4.7), (4.10), and (4.11), we find that

$$\int_a^b \left[r\left(\frac{dV}{dr}\right)^2 + \frac{\sigma^2}{r^3} V^2(r) \right] dr = \frac{1}{2}\left(1+\frac{\sigma^2}{|\sigma_c|^2}\right)\left[x^2\left(\frac{dV}{dx}\right)^2 \right]_{x=q_\lambda}^{x=\lambda q_\lambda}$$

$$= \frac{1}{2}\left(1+\frac{\sigma^2}{|\sigma_c|^2}\right) q_\lambda^2 [\lambda^2 \{Y_0(\lambda q_\lambda)J_1(\lambda q_\lambda) - J_0(\lambda q_\lambda)Y_1(\lambda q_\lambda)\}^2$$

$$- \{Y_0(\lambda q_\lambda)J_1(q_\lambda) - J_0(\lambda q_\lambda)Y_1(q_\lambda)\}^2]. \tag{4.12}$$

It is known that [19], 9.1.16

$$Y_0(\eta)J_1(\eta) - J_0(\eta)Y_1(\eta) = \frac{2}{\pi\eta}. \tag{4.13}$$

Applying this result reveals that

$$q_\lambda^2 \lambda^2 \{Y_0(\lambda q_\lambda)J_1(\lambda q_\lambda) - J_0(\lambda q_\lambda)Y_1(\lambda q_\lambda)\}^2 = \frac{4}{\pi^2}. \tag{4.14}$$

Also, since q_λ is a root of the determinant in Eq. (3.19) (and assuming $J_0(q_\lambda) \neq 0$),

$$Y_0(\lambda q_\lambda) = J_0(\lambda q_\lambda)\frac{Y_0(q_\lambda)}{J_0(q_\lambda)}. \tag{4.15}$$

This substitution allows the following term from Eq. (4.12) to be calculated as

$$q_\lambda^2 \{Y_0(\lambda q_\lambda)J_1(q_\lambda) - J_0(\lambda q_\lambda)Y_1(q_\lambda)\}^2$$

$$= q_\lambda^2 \frac{J_0^2(\lambda q_\lambda)}{J_0^2(q_\lambda)} [J_1(q_\lambda)Y_0(q_\lambda) - Y_1(q_\lambda)J_0(q_\lambda)]^2$$

$$= \frac{4}{\pi^2}\frac{J_0^2(\lambda q_\lambda)}{J_0^2(q_\lambda)}, \tag{4.16}$$

this last step being accomplished by another application of the result in Eq. (4.13). Insertion of Eqs. (4.16) and (4.14) into Eq. (4.12) now allows the full evaluation of ΔW in Eq. (4.6) to be given as

$$\Delta W = \frac{1}{\pi}\frac{u_0^2 \overline{B}}{Y_0^2(\lambda q_\lambda)}\frac{1}{|\sigma_c|^2}(|\sigma_c|^2 + \sigma^2)\left[1 - \frac{J_0^2(\lambda q_\lambda)}{J_0^2(q_\lambda)}\right]. \tag{4.17}$$

We now prove that $1 - J_0^2(\lambda q_\lambda)/J_0^2(q_\lambda)$ is positive for any $\lambda > 1$. Substituting for $Y_0(q_\lambda)$ from Eq. (4.15), it is seen that

$$J_0^2(q_\lambda) + Y_0^2(q_\lambda) = \frac{J_0^2(q_\lambda)}{J_0^2(\lambda q_\lambda)}[J_0^2(\lambda q_\lambda) + Y_0^2(\lambda q_\lambda)]. \tag{4.18}$$

Hence there is the equality

$$\frac{J_0^2(\lambda q_\lambda)}{J_0^2(q_\lambda)} = \frac{M_0^2(\lambda q_\lambda)}{M_0^2(q_\lambda)}, \tag{4.19}$$

where M_0, defined for any $\eta > 0$ by

$$M_0^2(\eta) = J_0^2(\eta) + Y_0^2(\eta), \tag{4.20}$$

is the usual modulus function for Bessel functions. The above result in Eq. (4.19) is not true in general, but depends on the fact that q_λ is a zero of the determinant in Eq. (3.19). It is well known (Ref. [20], p. 446) that $M_0^2(\eta)$ is a positive and strictly decreasing function for $\eta > 0$. Hence, since $\lambda > 1$, it is easily seen from Eq. (4.19) that

$$1 - \frac{J_0^2(\lambda q_\lambda)}{J_0^2(q_\lambda)} > 0. \tag{4.21}$$

It now follows from Eqs. (4.21) and (4.17) that $\Delta W < 0$ whenever $-\sigma^2 > |\sigma_c|^2$, that is,

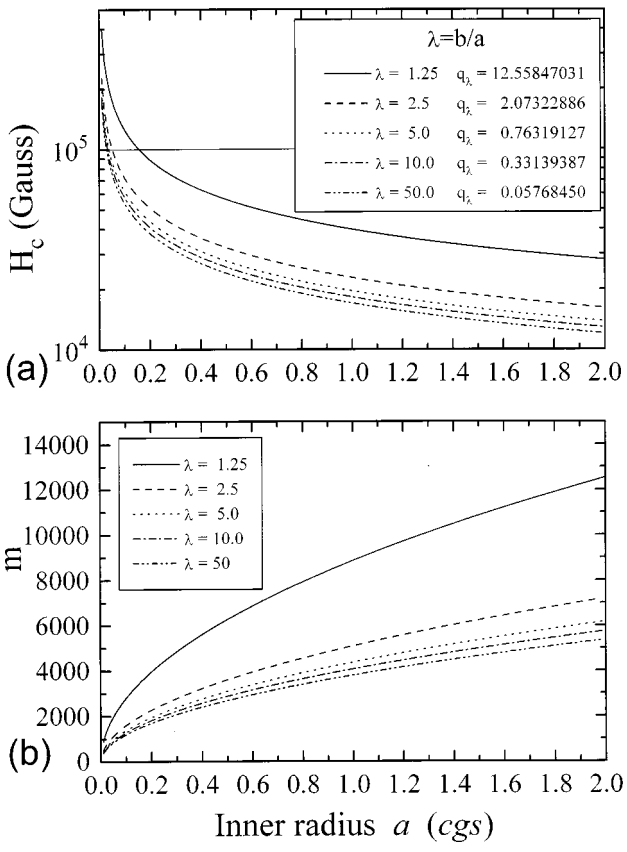

FIG. 2. The critical threshold H_c (G) for the onset of layer distortions is shown in (a) for $10^{-2} \leq a \leq 2$ (cm) for the particular physical parameters in Eq. (5.1) [the vertical axis in (a) is on a $\log_{10}$ scale]. Values for H_c have been calculated for the sample radius ratios λ, as indicated. The relevant zeros q_λ of determinant (3.19) are also given. The linked wave numbers m at H_c are given in (b) for the same values of λ.

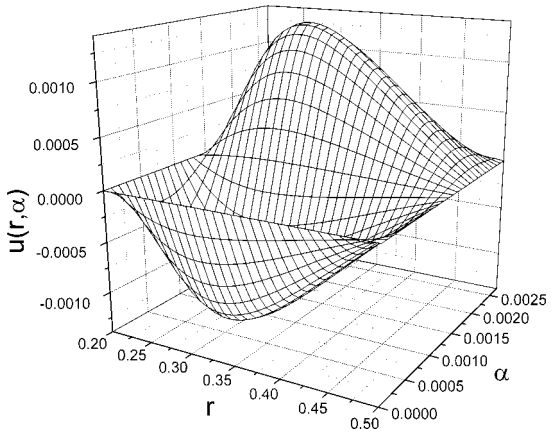

FIG. 3. Plot of $u(r,\alpha)$ for $a=0.2$ and $b=0.5$ (i.e., $\lambda=2.5$) and the physical parameters in Eq. (5.1) (in cgs units). In this case $H_c=50907$ (G), and the solution is plotted for the ranges $a\leqslant r\leqslant b$ and $0\leqslant\alpha\leqslant 2\pi/m$ (radians), m given by Eq. (5.3). The constant u_0 in Eq. (3.26) is set to 3×10^{-3} (1% of the radial depth $b-a$). The plot should be repeated m times in the α direction for a full representation of $u(r,\alpha)$.

$$\Delta W<0 \quad \text{whenever } H>H_c, \tag{4.22}$$

with H_c defined by Eq. (3.25) [employing Eq. (3.20)]. It is therefore expected that the variable solution $u(r,\alpha)$ will be preferred to the solution $u\equiv0$ for $H>H_c$.

V. EXAMPLES

We consider the physical values (in cgs units) (Ref. [3], p. 363)

$$K_1=10^{-6}, \quad \chi_a=10^{-7}, \quad \bar{B}=2.5\times10^{7}, \tag{5.1}$$

and plot the dependence of H_c (Gauss) upon the inner radius a for given cylindrical samples with radius ratios $\lambda=b/a$. For convenience, $\lambda=1.25$, 2.5, 5, 10, and 50 are chosen since the zeros of det(λ,q) are known from tables (Ref. [19], p. 415), and we consider feasible values for a by restricting it to the range $10^{-2}\leqslant a\leqslant 2$. The relevant Q_λ in Eq. (3.22) can then be calculated, which in turn allows H_c in Eq. (3.25) to be evaluated. The resulting graphs are shown in Fig. 2(a). The corresponding values for m in Eq. (3.28), which indicate the numbers of undulations, is a function of Q_λ and can be evaluated similarly leading to the plots in Fig. 2(b); from Eqs. (3.22) and (3.23) it is clear that $m\approx L\sqrt{a}$ for some constant L when $\lambda>1$ is fixed. For a given sample radius ratio λ and inner radius a, the corresponding m and H_c can be found from such graphs, and hence $|\sigma_c|$ in Eq. (3.27) can be calculated: this allows the calculation of the complete solution $u(r,\alpha)$ at the critical threshold H_c. From the figure, it is seen that H_c decreases as a and/or λ increases; m increases as a increases but decreases when λ increases.

Figure 3 shows the solution $u(r,\alpha)$ in Eq. (3.26) for the particular values

$$\lambda=2.5, \quad a=0.2, \quad b=0.5, \tag{5.2}$$

with the physical parameters in Eq. (5.1). In this case we find

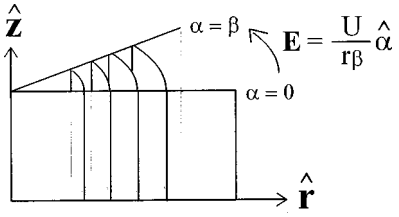

FIG. 4. The wedge geometry described in the text. The magnetic field shown in Fig. 1 is replaced by an electric field given by Eq. (6.2) applied across the boundaries at $\alpha=0$ and $\alpha=\beta$.

$$q_\lambda=2.073\,228\,86, \quad m=2276, \quad H_c=50\,907,$$
$$\sigma_c=1.036\,614\,43, \tag{5.3}$$

and set $u_0=3\times10^{-3}$ (that is, we choose to set the arbitrary small constant u_0 to 1% of the radial depth $b-a$). For clarity the solution is plotted for $a\leqslant r\leqslant b$ but with $0\leqslant\alpha\leqslant 2\pi/m$: the figure is repeated m times in the α direction to obtain the full representation of the displacement u at H_c. The critical current can easily be obtained from the results for the magnetic field by simply converting to appropriate units for current using tables, for example those contained in Abraham and Becker (Ref. [21], p. 251).

A comparison with the results for planar smectic-A samples is possible if we consider large radius a and small radial ratio $\lambda=b/a\approx1$. In these circumstances we have (Ref. [19])

$$m_c\approx Q_\lambda^{1/4}, \quad q_\lambda\approx\frac{\pi}{\lambda-1}, \tag{5.4}$$

and hence

$$\chi_a H_c^2\approx\chi_a f^2(m_c)\approx\frac{2}{a^2}K_1Q_\lambda^{1/2}=2\frac{b}{a^2}q_\lambda\sqrt{K_1\bar{B}}\approx2\frac{\pi}{d}\sqrt{K_1\bar{B}}, \tag{5.5}$$

where $d=b-a$. The approximation in Eq. (5.5) is identical to the result for planar samples (the notation λ in Ref. [3], p. 363 represents $\sqrt{K_1/\bar{B}}$). Thus the results in this paper collapse for thin samples to those for the planar case when a is large and d is small. In fact, $H_c\approx60$ kG in Ref. [3], and so the results presented above are in line with those elsewhere.

VI. CYLINDRICAL WEDGE UNDER AN ELECTRIC FIELD

The results presented above can be easily reinterpreted for the problem of an electric field applied across concentric cylindrical smectic-A layers. Here the geometry is identical to that in Fig. 1 except that $0\leqslant\alpha\leqslant\beta$ for some fixed ''wedge'' angle β. The magnetic field is replaced by an electric field E which follows the plane of the layers and is applied between bounding plates at $\alpha=0$ and $\alpha=\beta$, as depicted in Fig. 4. This particular wedge geometry has been extensively considered in the articles by Carlsson, Stewart, and Leslie [13] and Atkin and Stewart [14] in the context of smectic-C Freedericksz transitions. The results here predict critical voltage magnitudes U_c for an Helfrich-Hurault transition to occur for various wedge angles β.

Solutions are sought such that the ansatz in Eq. (3.1) can be employed again. To satisfy the zero boundary conditions at the plates, we set $m=\pi/\beta$. In this case we have that

$$u(r,\alpha)=v(r)\sin\left(\frac{\pi}{\beta}\alpha\right), \tag{6.1}$$

to which is added the zero boundary conditions on v in Eq. (3.2). The equations in Sec. II are changed using the substitutions (Ref. [3], p. 135) (see also Refs. [13], [14])

$$\mathbf{H}\rightarrow\mathbf{E}=\frac{U}{r\beta}\hat{\boldsymbol{\alpha}}, \quad \chi_a\rightarrow\frac{\epsilon_a}{4\pi}, \quad Ha\rightarrow\frac{U}{\beta}, \tag{6.2}$$

where U is the applied voltage, and the dielectric anisotropy ϵ_a is assumed positive. Equations (3.4) and (3.5) are the same except that $\sigma^2(m,H)$ is replaced by

$$\sigma^2(U)=\frac{\pi^2}{\beta^4}\frac{1}{\overline{B}}\left(K_1(\pi^2-\beta^2)-\frac{\epsilon_a}{4\pi}U^2\right). \tag{6.3}$$

For $\sigma^2(U)\geqslant 0$ the arguments in case (i) after Eq. (3.5) again show that $v(r)\equiv 0$ is the only solution available. Following through the argument in case (ii) shows that when $\sigma^2(U)<0$ a nonzero solution can be obtained for $v(r)$, provided

$$b^2q_\lambda^2=-\sigma^2(U)=\frac{\pi^2}{\beta^4}\frac{1}{\overline{B}}\left(\frac{\epsilon_a}{4\pi}U^2-K_1(\pi^2-\beta^2)\right) \tag{6.4}$$

with λ and q_λ defined as before. It follows from Eq. (6.4) that the critical voltage U_c is found to be

$$U_c=\left(\frac{4\pi K_1}{\epsilon_a}\right)^{1/2}\left(\pi^2-\beta^2+\frac{\beta^4}{\pi^2}Q_\lambda\right)^{1/2}, \tag{6.5}$$

Q_λ being given by Eq. (3.22). The rôles of β and the radius ratio λ are evident from the form of U_c in Eq. (6.5). Introducing

$$|\sigma_c|=|\sigma(U_c)|=bq_\lambda \tag{6.6}$$

results in the solution given by

$$u(r,\alpha)=u_0\frac{\sin\left(\frac{\pi}{\beta}\alpha\right)}{Y_0\left(\frac{|\sigma_c|}{a}\right)}V(r), \tag{6.7}$$

with $V(r)$ given by Eq. (3.26) with $|\sigma_c|$ appropriately redefined by Eq. (6.6). The energy argument in Sec. IV remains unchanged with the obvious modifications for the limits in α, resulting in

$$\Delta W<0 \quad \text{whenever} \quad U>U_c, \tag{6.8}$$

with U_c defined by Eq. (6.5). It is therefore expected, as in the magnetic field problem examined above, that the system will prefer the variable solution $u(r,\alpha)$ to the zero solution when the magnitude of the voltage exceeds U_c.

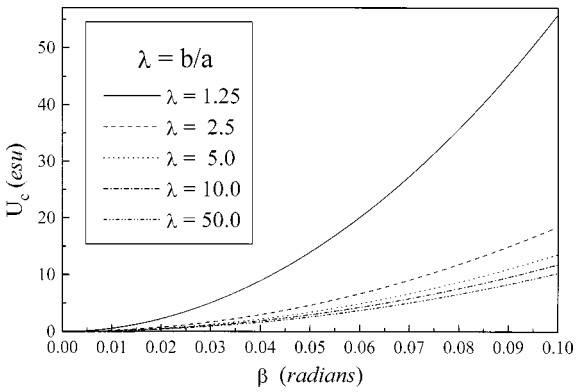

FIG. 5. Critical magnitudes U_c (statvolt) of the applied voltage for the radial ratios λ as indicated. The inner radius is fixed at $a=10^{-1}$ (cm) and $0\leqslant\beta\leqslant 0.1$ ($\approx 5.7°$). The physical constants K_1 and $\overline{B}$ are as in Eq. (5.1), while $\epsilon_a/4\pi$ has been set to 0.2.

Examples of critical applied voltages U_c (in esu units) are displayed in Fig. 5 for the same values of λ as in Fig. 2 above. The constants used are those in Eq. (5.1) except that χ_a is replaced by $\epsilon_a/4\pi=0.2$. The inner radius a is fixed to be 10^{-1} (cm), and the plots are for values of the wedge angle in the range $0\leqslant\beta\leqslant 0.1$ ($\approx 5.7°$): of course, any other values for ϵ_a, a, and β are possible, depending upon the application considered. This particular choice is of relevance for samples which have a low wedge angle, for instance a usual ''bookshelf'' geometry of layers with one end of the sample slightly narrower than the other (the arc lengths are βa^2 and βb^2 at the inner and outer radii, respectively). If the radial depth is defined to be $b-a$ then $\lambda=1.25$, 2.5, 5, 10, and 50 correspond to depths of 0.025, 0.15, 0.4, 0.9, and 4.9 (cm), respectively, when $a=10^{-1}$.

VII. CONCLUSIONS

It has been shown that an Helfrich-Hurault-type transition is theoretically possible for concentric cylindrical layers of smectic-*A* liquid crystal arranged as shown in Fig. 1. It is assumed that the anisotropy of diamagnetic susceptibility χ_a is positive. A magnetic field applied in the azimuthal direction $\hat{\boldsymbol{\alpha}}$ parallel to the layers induces layer distortions, analogous to those for planar aligned samples, when the magnitude of the field is greater than a critical value H_c, given by Eq. (3.25). The solution $u(r,\alpha)$ at the threshold value H_c has been derived explicitly in Eq. (3.26), and in Sec. IV it has been shown to be energetically favorable compared to the zero solution. The variable solution $u(r,\alpha)$ at $H=H_c$ has an r dependence given by Eq. (3.26) with a critical wave number m (in the α direction) given via Eqs. (3.23) and (3.28). For a given inner radius a and outer radius b the dependence of the critical behavior upon the ratio $\lambda=b/a$ has been examined: in particular, the critical threshold result for thin radial samples matches the threshold of the usual planar aligned samples when a is large, as shown by Eq. (5.5).

Section V investigated the results for the physical parameters in Eq. (5.1), and calculated the corresponding H_c for $10^{-2}\leqslant a\leqslant 2$, $\lambda=b/a=1.25$, 2.5, 5, 10, and 50 (cgs units). Linked with H_c is the corresponding wave number m, found from a minimization of the field strength H, as discussed in Sec. III. Graphs of H_c and m as functions of a and λ are

given in Fig. 2. Figure 2 provides useful guidance for the consideration of experimental setups with regard to the choices of inner and outer radii and the resulting possible critical thresholds and wavenumbers. It is clear from Fig. 2(a) that radially deeper samples always lead to lower thresholds. Figure 3 is a plot of a particular solution $u(r,\alpha)$ in Eq. (3.26) for the parameters in Eq. (5.1) with λ, a, and b given by Eq. (5.2); it is plotted for $a \leqslant r \leqslant b$ and $0 \leqslant \alpha \leqslant 2\pi/m$, as discussed in Sec. V. The figure displays the typical qualitative features of such solutions in general: in this particular example the resulting threshold is given in (5.3) as $H_c = 50\,907$ G, similar to that reported for planar samples.

The results for a magnetic field were extended to an electric field for the wedge geometry discussed in Sec. VI. The dependence of the critical applied voltage U_c upon the wedge angle β is given by Eq. (6.5), and plots of U_c are displayed in Fig. 5 for the physical parameters used before, except that χ_a is replaced by $\epsilon_0/4\pi = 0.2$. These results are particularly relevant for samples close to a ''bookshelf'' geometry when β is small (in Fig. 5, $0 \leqslant \beta \leqslant 5.7°$). In the degenerate case of $\beta = 0$, which is of course physically unrealistic because the sample would have zero volume, it should nevertheless be observed that U_c in Eq. (6.5) becomes

$$U_c = \pi \left(\frac{4\pi K_1}{\epsilon_a} \right)^{1/2}. \tag{7.1}$$

With the obvious change in notation $\epsilon_a \rightarrow 4\pi\epsilon_0\Delta\epsilon$, this is exactly the critical voltage mentioned by Elston [22] for the usual Fréedericksz transition in nematic liquid crystals. Elston went on to discuss layer distortions in planar smectic-*A* bookshelf layers, and found a critical voltage when the sample is close to T_{AC} which is identical to that derived by Kedney and Stewart [23] for the lowest order sine mode for layer deformations in smectic-*C* layers: this critical threshold voltage is twice that given by Eq. (7.1). A direct comparison with the work in Ref. [22] and the wedge results presented here seems to indicate that an experiment of the type proposed for cylindrical smectic-*A* layers ought to have a lower critical voltage for layer distortions than that for planar layers when the wedge angle β is small. Consideration of the factors discussed in this paper will hopefully stimulate further discussion and interest in possible Helfrich-Hurault transitions for smectic liquid crystals.

[1] W. Helfrich, J. Chem. Phys. **55**, 839 (1971).
[2] J. P. Hurault, J. Chem. Phys. **59**, 2068 (1973).
[3] P. G. de Gennes and J. Prost, *The Physics of Liquid Crystals* (Clarendon, Oxford, 1993).
[4] S. Chandrasekhar, *Liquid Crystals*, 2nd ed. (Cambridge University Press, Cambridge, 1992).
[5] W. Bragg, Nature (London) **133**, 445 (1934).
[6] M. Nakagawa, J. Phys. Soc. Jpn. **59**, 81 (1990).
[7] F. M. Leslie, I. W. Stewart, and M. Nakagawa, Mol. Cryst. Liq. Cryst. **198**, 443 (1991).
[8] M. Kleman, J. Phys. (Paris) **38**, 1511 (1977).
[9] C. S. Rosenblatt, R. Pindak, N. A. Clark, and R. B. Meyer, J. Phys. (Paris) **38**, 1105 (1977).
[10] I. W. Stewart, Liq. Cryst. **15**, 859 (1993).
[11] I. W. Stewart, F. M. Leslie, and M. Nakagawa, Q. J. Mech. Appl. Math. **47**, 511 (1994).
[12] R. J. Atkin and I. W. Stewart, Q. J. Mech. Appl. Math. **47**, 231 (1994).
[13] T. Carlsson, I. W. Stewart, and F. M. Leslie, Liq. Cryst. **9**, 661 (1991).
[14] R. J. Atkin and I. W. Stewart, Liq. Cryst. **22**, 585 (1997).
[15] P. Das and W. H. Schwarz, Phys. Rev. E **51**, 3588 (1995).
[16] M. Kleman and O. Parodi, J. Phys. (Paris) **36**, 671 (1975).
[17] I. W. Stewart, Phys. Rev. E **58**, 5926 (1998).
[18] V. I. Smirnov, *A Course of Higher Mathematics* (Pergamon, Oxford, 1964), Vol. 4.
[19] *Handbook of Mathematical Functions*, edited by M. Abramowitz and I. A. Stegun (Dover, New York, 1970).
[20] G. N. Watson, *A Treatise on the Theory of Bessel Functions*, 2nd ed. (Cambridge University Press, Cambridge, 1966).
[21] M. Abraham and R. Becker, *Electricity and Magnetism* (Blackie, Glasgow, 1948).
[22] S. J. Elston, Phys. Rev. E **58**, R1215 (1998).
[23] P. J. Kedney and I. W. Stewart, Z. Angew. Math. Phys. **45**, 882 (1994).